



# PACIFIC REGION TECHNICAL NOTES

79-018

June 18, 1979

## Further Examination of New TIROS-N Sounding Data

Pat Morin, Meteorologist  
Pacific Weather Centre, Vancouver

---

### INTRODUCTION

It is becoming apparent that lack of data is seriously hampering the potential of higher resolution models especially over the oceans and the west coast. As a result satellite data is assuming more importance. For several years, satellite data (16) in the form of vertical temperature and/or thickness profiles (VTPR) have been available to the Pacific Weather Center. Since February, data from a new generation of satellites (TIROS-N) is now available (see Pacific Region Technical Note 79-010, Horita and Spagnol). As a follow up to Note 79-010, one month of satellite data is examined. The following is a brief discussion on data distribution and quality, and it's potential use to the forecasters of PAWC. Appendix A contains a very brief look to the background and technology involved in the use of satellites to retrieve atmospheric radiances.

### EXAMINATION OF DATA

#### SPATIAL AND TEMPORAL DISTRIBUTION

A month of data (1879 reports) from March 15 to April 15, 1979 was examined. Figure 5a gives the distribution of the reports over the eastern Pacific while fig. 5b gives the longitudinal percentage distribution of reports. Figure 5c gives the percentage distribution of reports centered about the main synoptic hours  $\pm 3$ . The concentration of reports about 00Z may be due to satellite orbit characteristics which result in the data being closer to 00Z window than 06Z. The characteristics of polar orbits result in much overlapping at the poles but undercoverage at the equator. Hence there should be a drop in reports per unit area towards the equator. The drop in VTPR's at 60N in fig. 5b is deliberate due to the extensive orbit overlapping as one approaches the pole.

Of the 1879 reports, 913 (49%) were in a usable area outlined in fig. 5a. The VTPR density in a 12 hour period was found to be 40% of that provided by radiosondes located N of 50N and W of 150W - i.e. about 1 VTPR per  $41 \text{ long deg}^2$ . When one considers that we have only 1 sounding (C7P) over the eastern Pacific, the VTPR's should be a welcomed asset, albeit not as detailed as regular radiosondes.

### ACCURACY OF THE VTPR 500 MB Thickness

Over the continent, temporal and spatial fields of the 500 mb thickness fields are available so that VTPR taken over the areas of interest can be compared with actual values derived from a number of radiosondes. Such fields are not available with any degree of accuracy over the eastern Pacific due to lack of data and smoothing of the data. Hence, it was necessary to derive the expected 500 mb thickness by using satellite pictures, various NWP products and standard practices to take into account system movements.

Of 913 reports 98 were examined to determine the accuracy of the VTPR 500 mb thickness. A VTPR was examined if it was found to be within 2,3 long deg and 3 hours of a nearby radiosonde. If a VTPR value was within 2 DKM, then it was considered correct as this is considered the limit of radiosonde accuracy (19). If a report deviated by 3 DKM or more after all careful examination of the facts, then it was assumed to be in error by at least 2 DKM or higher.

Of the 98 reports examined, 25 were considered biased with an RMS of 4 DKM vs. 2 DKM for the whole data set of 98 VTPR's. The RMS for the data set is similar to that found in a previous study (16) using NOAA 2 data. In this study the RMS was found to range from 2.2C to 1.5C. For the new TIROS-N, the RMS is expected to approach 1.5C. (A 1C° difference in an air column, say between 500 mb and 700 mb, is equivalent to 1 DKM difference.)

From the 25 reports determined to be biased, 14 gave a mean error of +3.6 DKM and 11 of -3.7 DKM. From the 98 VTPR examined, 31 reports were located about the weather ship C7P (fig. 6). The RMS for this set was 2.3 DKM but considering the 10 biased reports the RMS was 4 DKM similar to the RMS determined for all biased reports. The average negative and positive bias was -4.5 DKM and +3.7 DKM.

The RMS determined for the VTPR's taken about the weather ship with no considerations given to system movements was found to be +3.1 DKM.

It becomes obvious that more than a quick perusal is required to determine whether a report is biased. Reference (18) gives a good summary of the sources of errors inherent in the methods used to retrieving temperatures from radiances.

What can be used to determine if a VTPR is biased? For the 31 reports about the weather ship, the moisture distribution in the significant layers 500-700 mb, etc, was noted along with synoptic data and frontal systems. Two additional parameters provided by TIROS-N were also provided - precipitable water and the confidence factor. The precipitable water was no help in discriminating a biased report as a warm dry airmass can contain as much moisture as a colder moist airmass. I suspect that precipitable water serves more as a correction factor in determining the values of the transmittance required for temperature retrieval. As yet, PAWC is still waiting for detailed information with regards to the methods of deriving thickness values from radiance

observed by TIROS-N. The confidence factor was found to be equally disappointing. Knowledge of the synoptic pattern and moisture distribution were better guides as better readings were found to exist under upper ridges (fig. 7) but not always. This is to be expected as the sensor will work best in clear air columns.

Many VTPR were in error in cloud and precipitation situations but not always. No definite method was found to help differentiate a positive from a negative bias. Figure 8 and 9 are examples of two synoptic situations which gave the largest biases; +8 and -8 DKM. The profiles associated with these errors should not be construed as being typical patterns that gave positive or negative biases. Figure 10 illustrates the corresponding satellite photos and 500 mb height and thickness field with the VTPR position by a \* and the value in brackets.

#### APPLICATION

The first generation of satellite data (SIRS) was used by the British (7), Israeli, Australian (9) and other weather services with success. This is now followed by data derived by the new Tiros-N. The main problems encountered with using this sort of data was accuracy of data and data assimilation techniques (10, 11) as mathematical techniques do not give a unique solution and much of the data is asynoptic - i.e. at times other than 00Z, 12Z, etc. As the number of polar orbiting satellites used in retrieving VTPR's increase and assimilation techniques improve these problems will disappear. However, these problems need not detract from their immediate use in analysing vast areas of open ocean where forecast fields are often erroneous by many DKM. In addition to VTPR's, the Pacific Weather Center receives numerous airesps and satellite photos. An example of the use of VTPR as an aid to forecasting is demonstrated by the weather events as they unfolded during this year's Victoria Day weekend.

Prior to the Victoria Day weekend, various NWP products indicated generally sunny skies and no significant precipitation and PAWC forecasts for the weekend reflected this. An early Saturday morning satellite photo (fig. 11) hinted of a possible frontal wave south of C7P. Figure 12b shows the VTPR 500 mb thickness distribution. Figure 12a shows an interpolated 500 mb thickness field over the eastern Pacific centered about the 18z VTPR reports. The stippled area in fig. 12a outlines the 534-540 thickness ribbon obtained by interpolating between the actual analysis and the 12 hour LFM SFC-500th prog. Figure 13 is the LFM 500 mb height thickness analysis for 19/12z for the area in question. Fig. 14 shows the 24 hour forecast LFM 700 mb height field and the actual height field for 20/12z. On figure 12a, some airesps have been plotted. There were several airesps between 44-46N along 160W between 100-125 knots. Due to overlapping only 3 have been plotted. An examination of these winds and fig. 13 indicate a poor LFM analysis southwest of the weathership C7P. As well, the 534-540 thickness ribbon extends further to the southwest of the 18z LFM 534-540 ribbon and both winds and VTPR thickness corroborate the presence of a strong northwesterly flow of cold air to the southwest of the ship C7P. The conditions for development are favourable and subsequent satellite

photos show this. Continued development of an anticyclonic cirrus shield, indicative of a developing low, signalled Vancouver forecasters to call for a wetter weekend. Figures 11b and c show the subsequent movement of the low which gave significant precipitation to some areas of B.C. Figure 14 clearly shows the discrepancy between the forecast and actual circulation Sunday morning May 20 just off the B.C. coast.

#### CONCLUSIONS

The analysis of the TIROS N data has revealed that data distribution over the eastern Pacific is good during any 12 hour period. The data was found to have an RMS of 2 DKM however, 25% of the data was found to be biased by several DKM with individual errors as high as  $\pm 8$  DKM.

\*\*\*\*\*

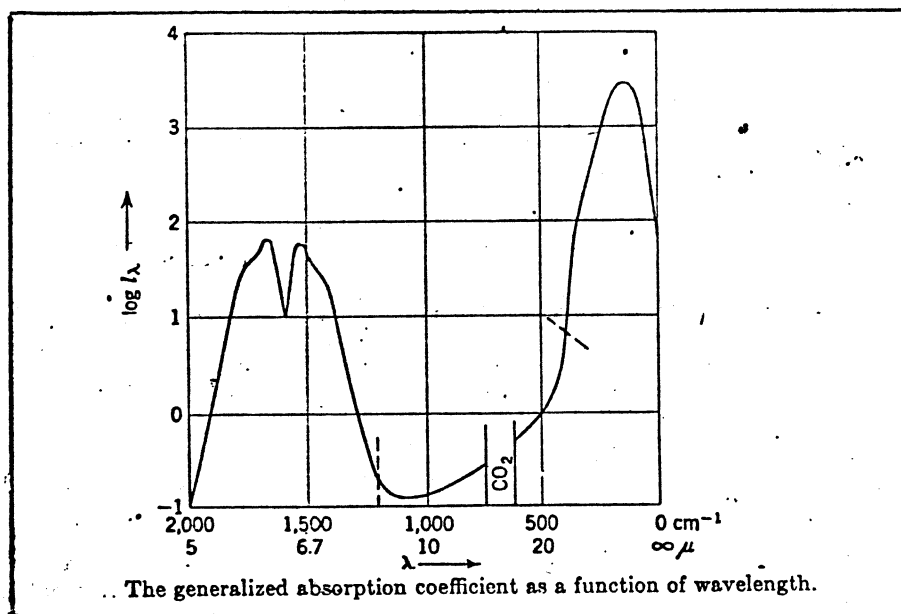


FIG. 1

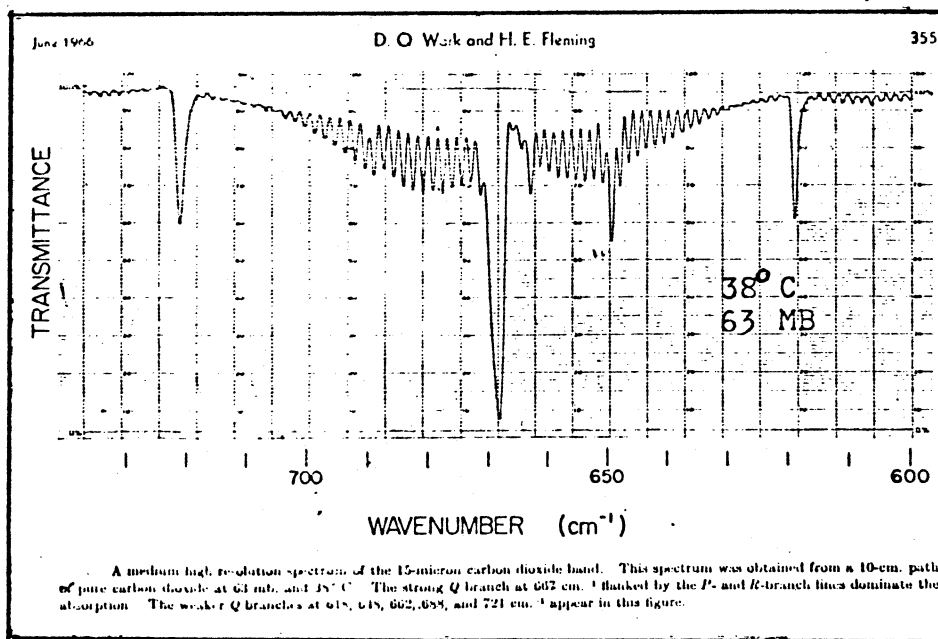
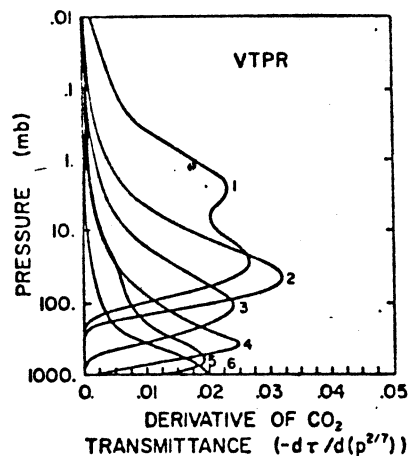


FIG. 2

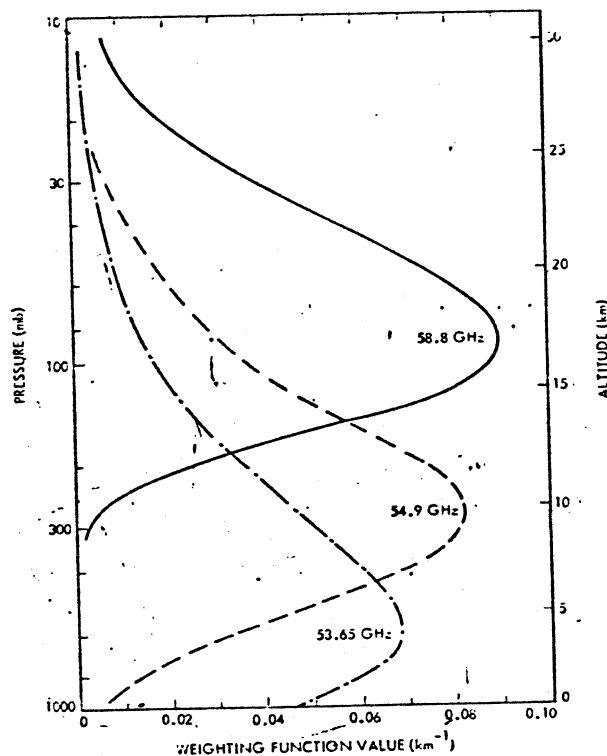
TABLE 1. NOAA VTPR channels.

Channel no.	Wavelength ( $\mu\text{m}$ )	Wavenumber ( $\text{cm}^{-1}$ )	Approximate peak level of weighting function (mb)
CO <sub>2</sub> channels: 15 $\mu\text{m}$ CO <sub>2</sub> absorption band			
1 (Q branch)	14.96	668.5	30
2	14.77	677.5	50
3	14.38	695.0	120
4	14.12	708.0	400
5	13.79	725.0	600
6	13.38	747.0	surface
H <sub>2</sub> O channel: Rotational water vapor absorption band			
7	18.69	535.0	700
Window channel: Atmospheric window region			
8	11.97	833.0	surface



VTPR CO<sub>2</sub> channel weighting functions for U. S. Standard Atmosphere.

FIG. 3



NEMS temperature weighting functions calculated for the 1962 U. S. Standard Atmosphere and zero surface reflectivity.

FIG. 4

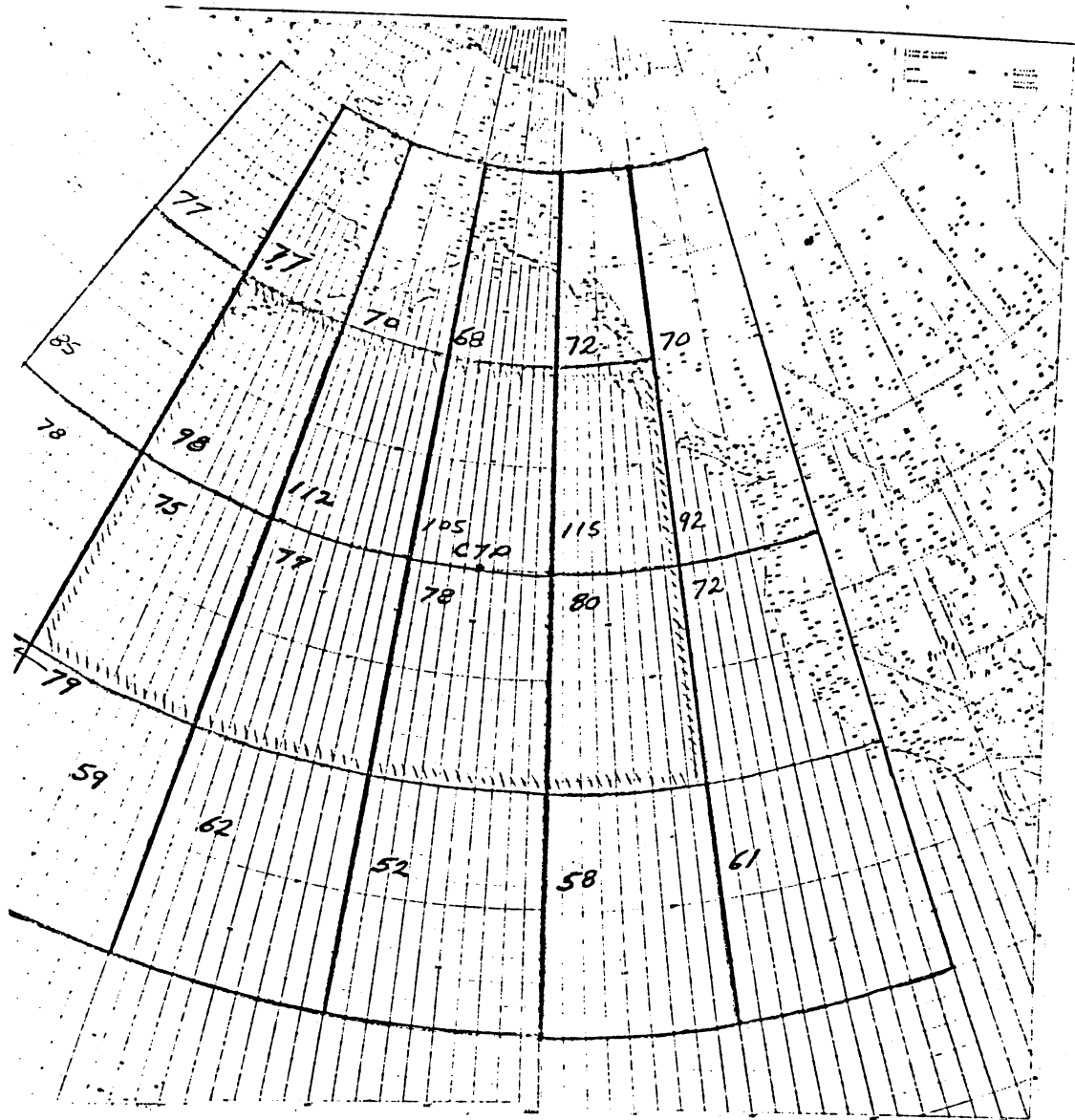


FIG. 5A THE DISTRIBUTION OF 1 MONTH OF VTPR REPORTS.

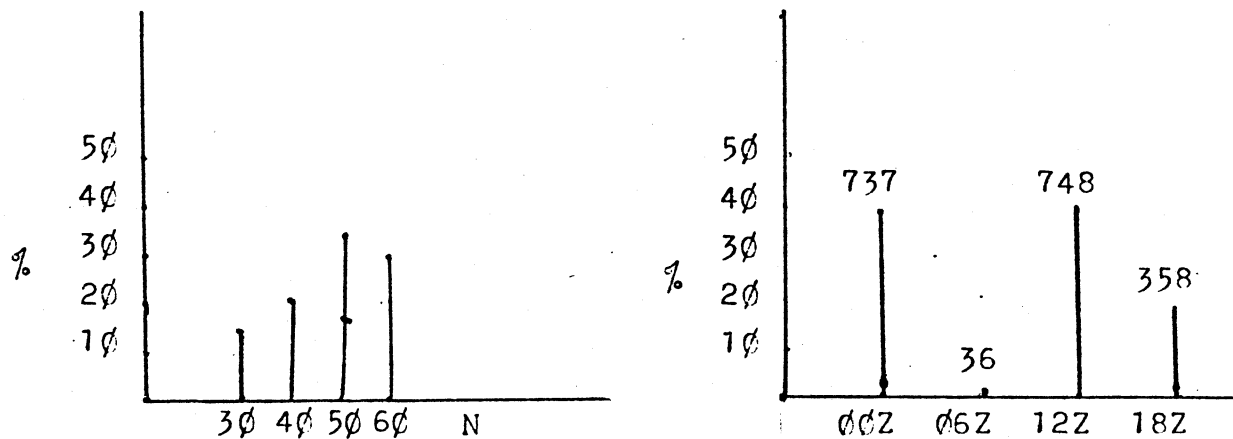


FIG. 5B, 5C LATITUDINAL DISTRIBUTION AND TIME DISTRIBUTION OF VTPR'S.

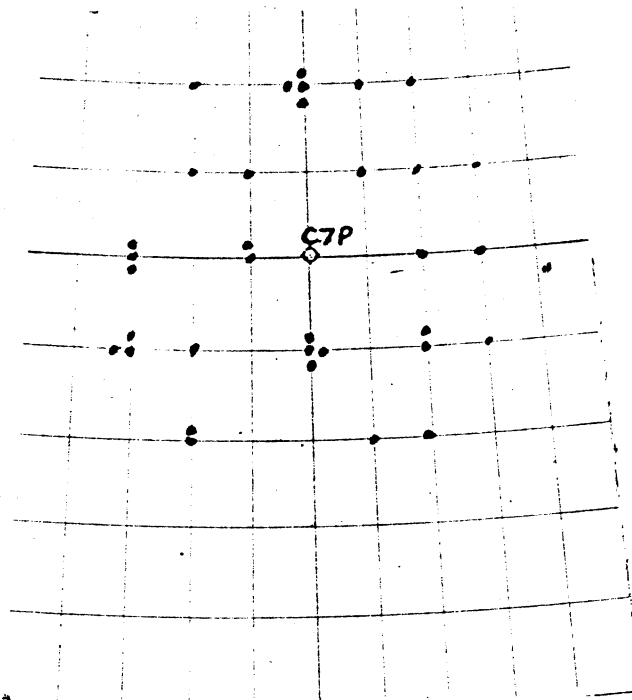


FIG.6 VTPR DISTRIBUTION FOR ONE MONTH ABOUT C7P.

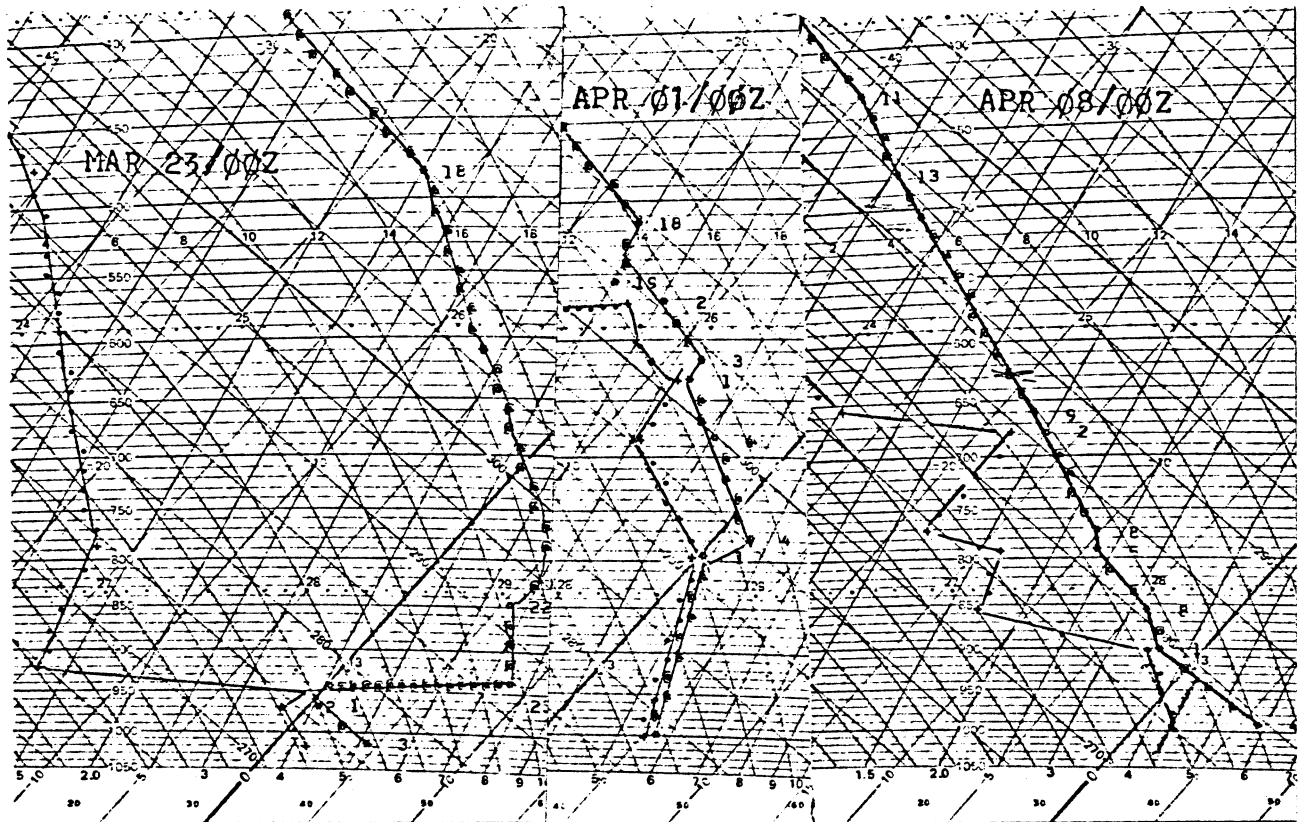


FIG.7. TYPICAL SOUNDING ASSOCIATED WITH HIGH FREQUENCY OF "CORRECT" VTPR'S.

FIG.8. SOUNDING NEAR A VTPR WITH +8DKM BIAS.

FIG.9. SOUNDING NEAR A VTPR WITH -8DKM BIAS.



2315 31MR79 35A-4 00402 18921 UC2

2315 07AP79 35A-4 00391 18981 UC2

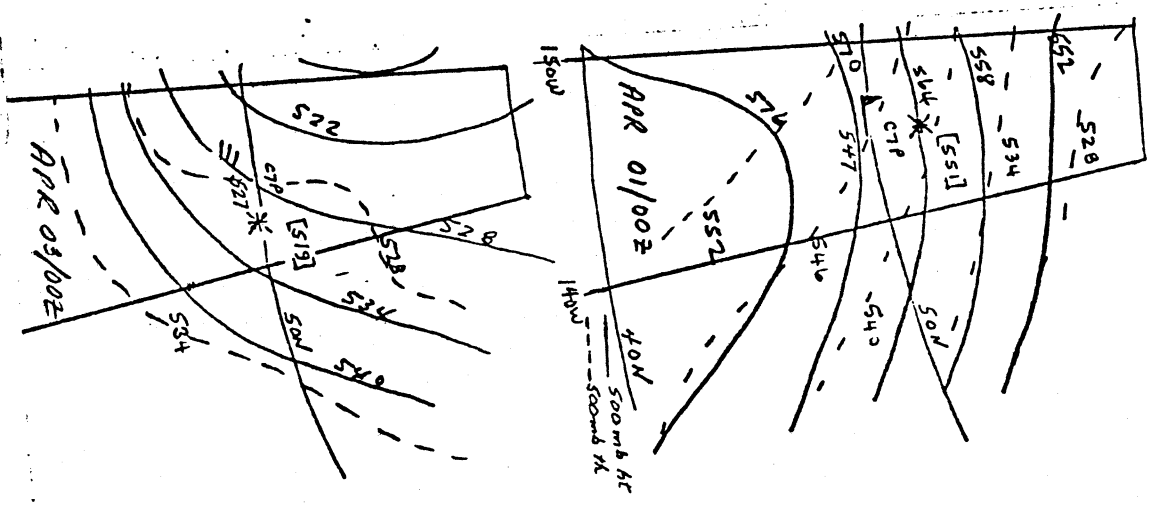
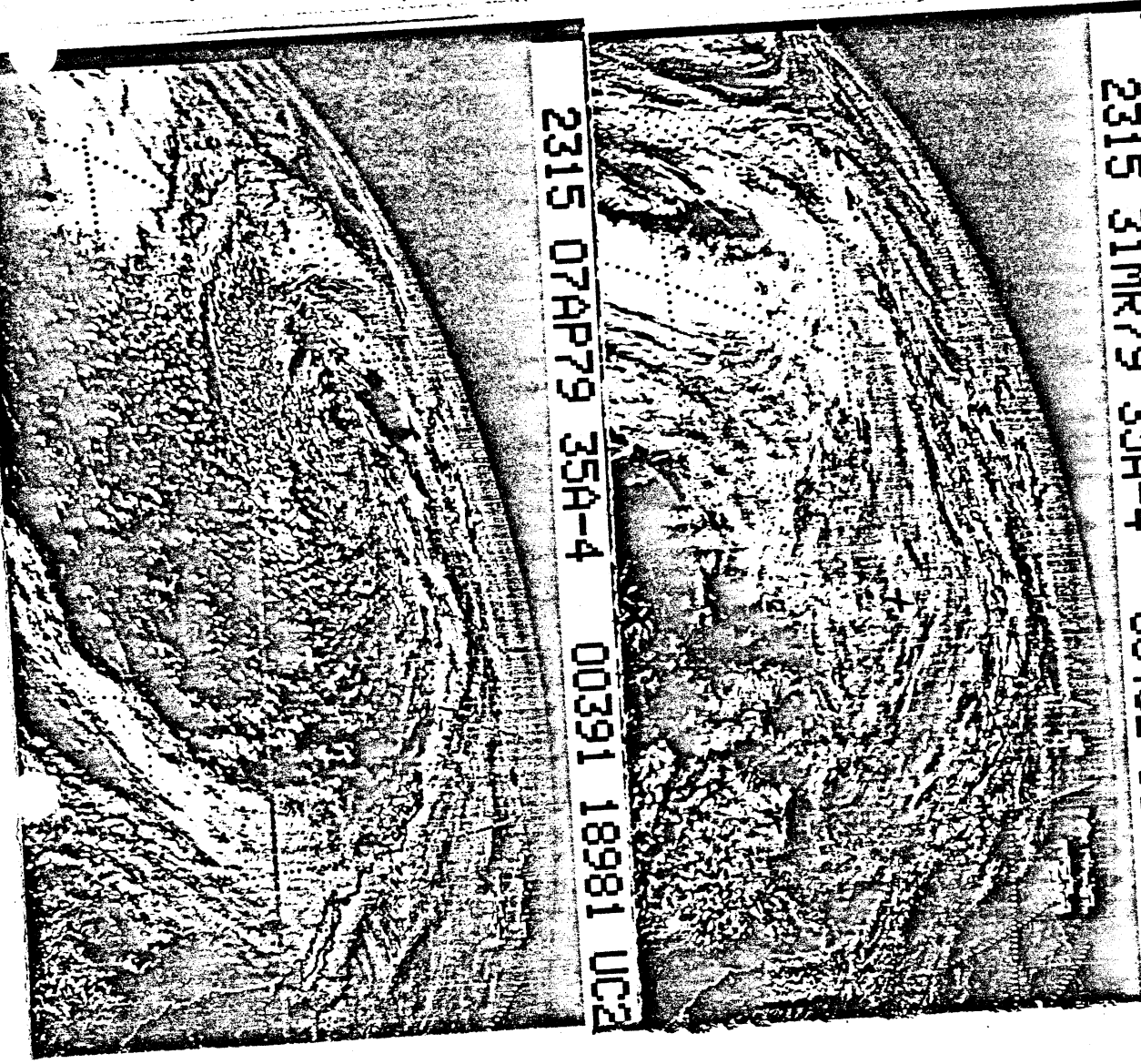


FIG. 1 Ø 500MB CMC THICKNESS  
HEIGHT FIELD AND CORRESPONDING  
SATELLITE PHOTOS. SATELLITE  
"VTPR" IN BRACKETS:



FIG.11A

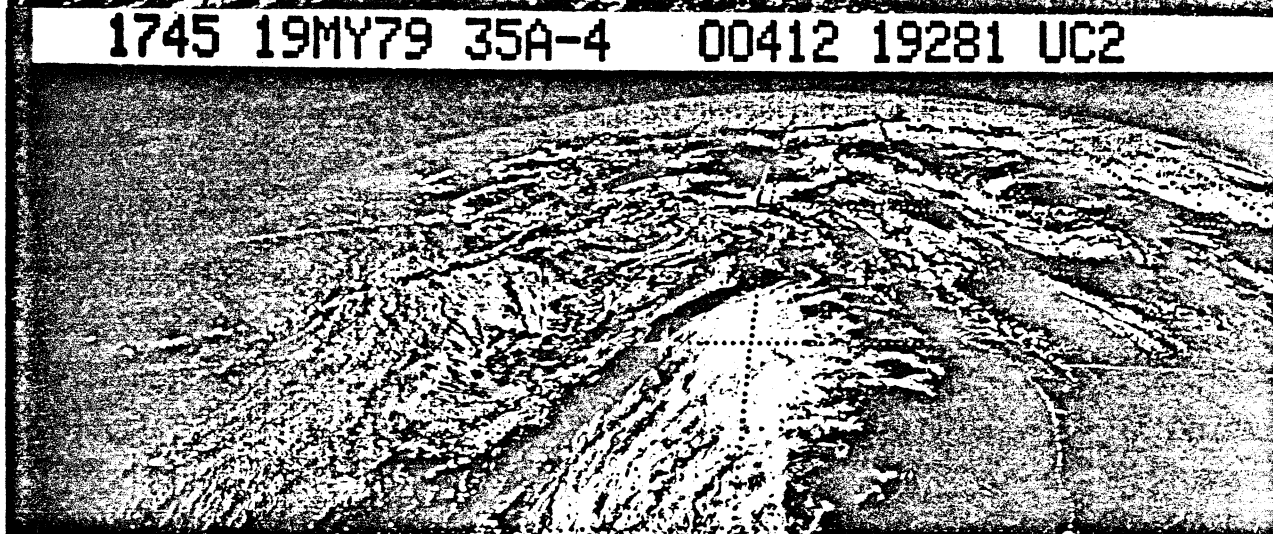


FIG.11B

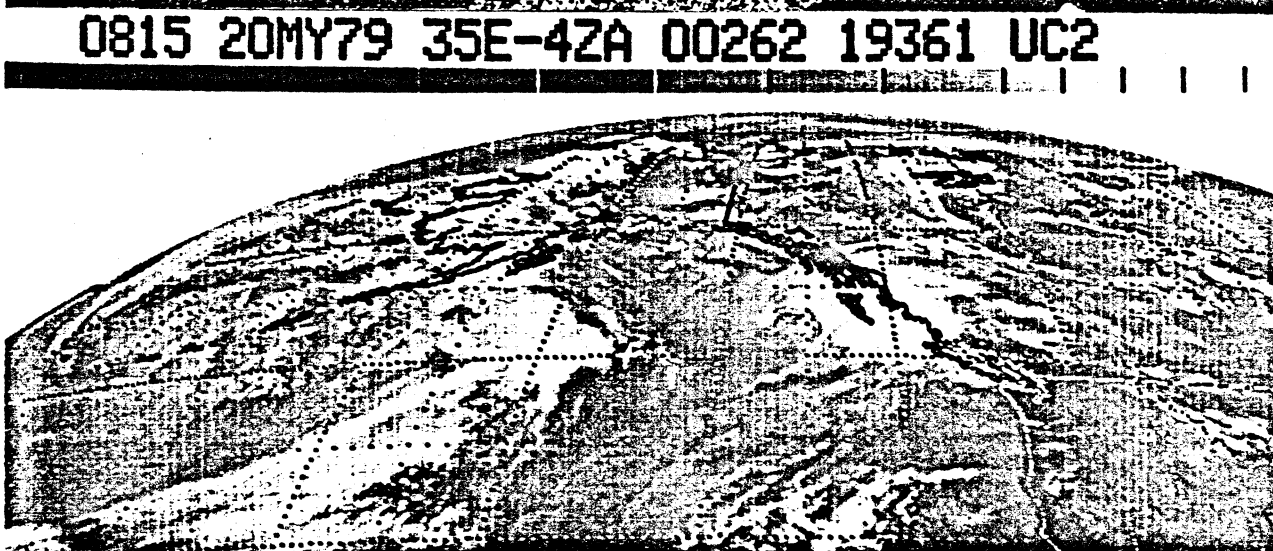


FIG.11C

FIG.11 PHOTOS SHOW DEVELOPING FRONTAL WAVE SOUTHWEST OF C7P AND IT'S SUBSEQUENT MOVEMENT INTO B.C.

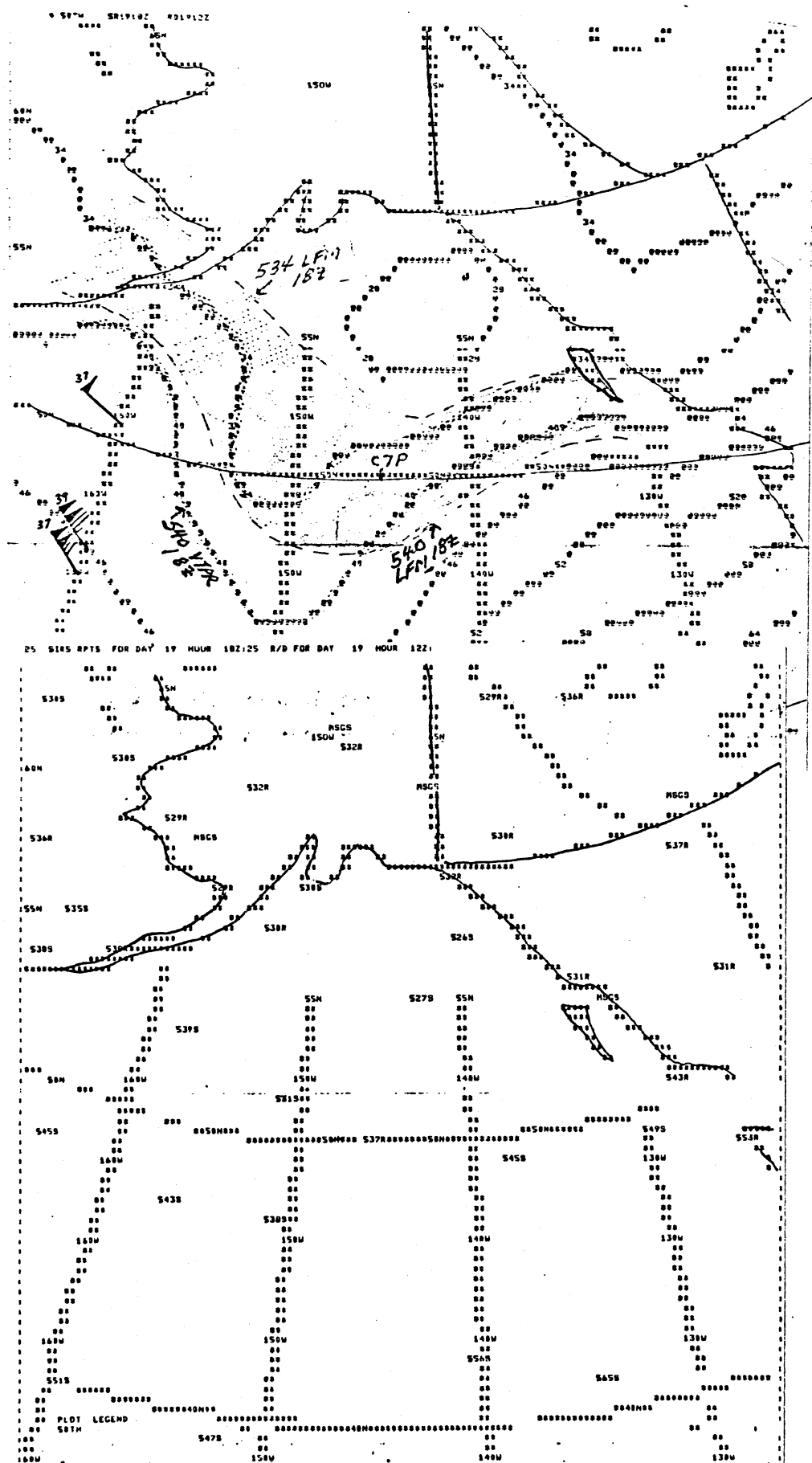


FIG.12A VTPR 500MB THICKNESS FIELD CENTERED ABOUT 18Z.  
FIG.12B VTPR DISTRIBUTION OVER EASTERN PACIFIC ABOUT 18Z  
AND LAND RADIOSONDES FOR 12Z.

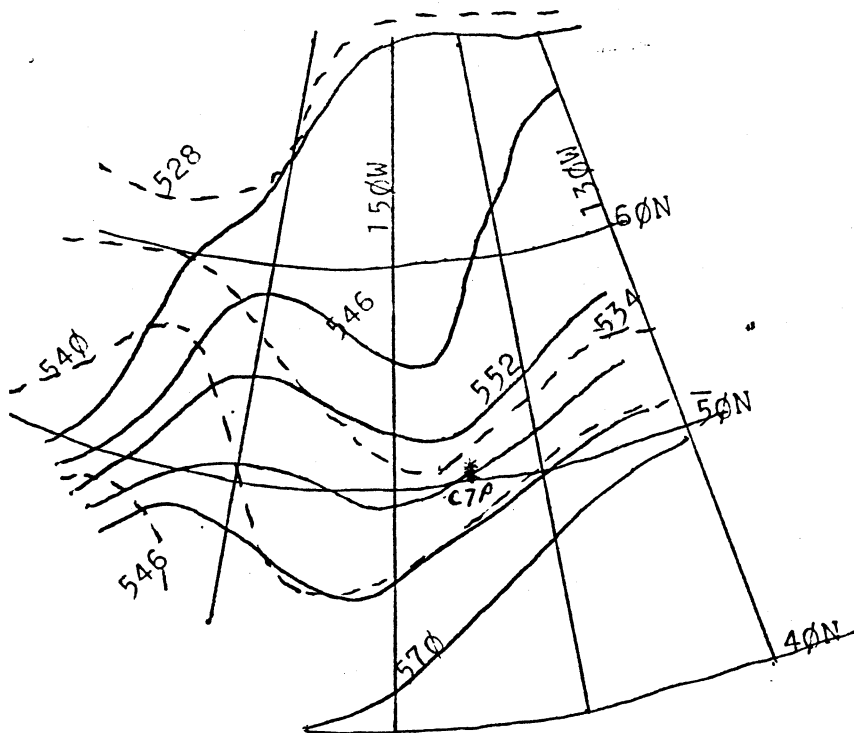


FIG. 13 LFM 500MB HT — AND 500MB TH ---  
FOR SAT. MAY 19/12Z 1979.

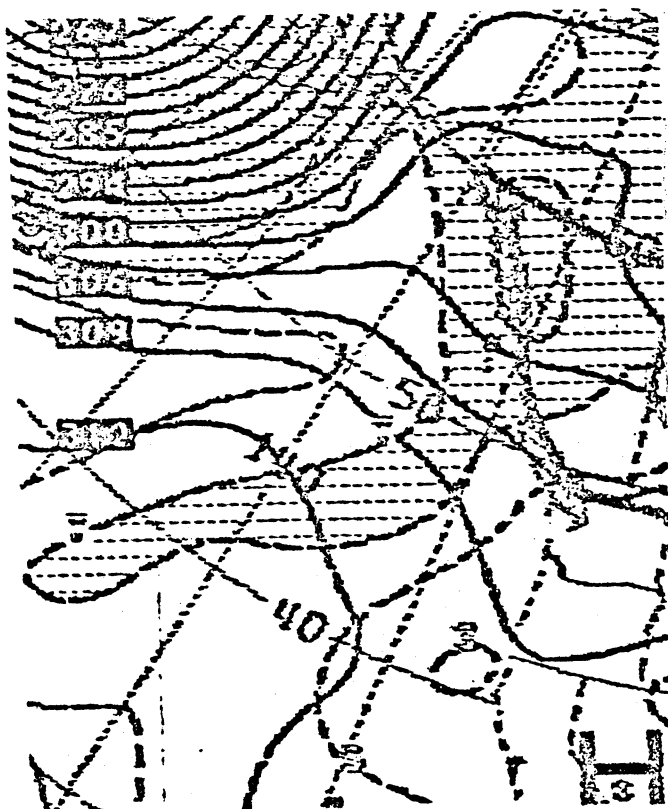
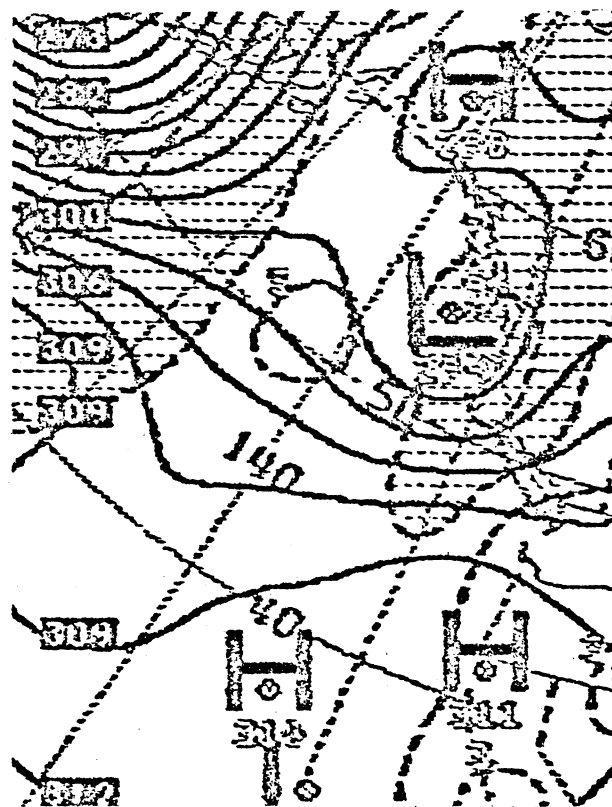


FIG. 14 LFM 700MB HEIGHT FORECAST  
FOR MAY 20/12Z.



LFM 700MB HEIGHT ACTUAL  
FOR MAY 20/12Z.

AUTHOR'S RECOMMENDATION FOR OPTIMIZING USAGE OF SATELLITE DATA

Due to the extensive number of synoptic reports over the continent, forecasters there can derive firm conclusions about impending developments using areas of PVA, PTA,  $\nabla V$ , etc. and can relate these to features in satellite photos with confidence. Due to lack of data and oversmoothing over the eastern Pacific, west coast forecasters are not so fortunate. Frequent disorganized cloud masses or lack of cloud along with the ageostrophic nature of the wind field (14, 19) in the everchanging atmosphere make it difficult to infer a good wind field with any degree of confidence. One must continually bear in mind the saying 'Believe half of what you see. On the other hand, PAWC receives much asynoptic data--aireps, satellite VTPR's, winds and photos which could be used advantageously. The lack of an attractive and coherent package that merges the data in a usable form for present and past analysis severely detracts from its usage by forecasters on a continual basis.

PAWC will receive more and more new forms of data, both synoptic and asynoptic. While there is much to be gained in putting resources in new "technological toys", let us not cast aside other types of old and proven data which can be used to corroborate new forms of data which are open to a multitude of interpretations. PAWC has now received satellite pictures on a half hourly basis for nearly three years, yet there has been little if any improvement in the verification scores of various PAWC products. It is essential PAWC or AES reallocate resources to fully utilize this data, i.e. possibly through cloud, wind, height, and thickness composites as produced by other meteorological services (9, 12, 13). Also, more time should be spent in developing more and better methods for man-machine interactive numerical models so that the time gap between new data forms and its automatic incorporation in numerical models narrows.

Hence the inherent ability of Homo Sapiens to recognize patterns, example data, and anticipate events, unforeseen by empirical models, can be utilized to adjust model outputs. As well, PAWC meteorologists can maintain a higher degree of professionalism by making a more scientific assessment of parameters rather than taking NWP products as fact.

REFERENCES

1. Indirect Measurements of Atmospheric Temperature Profiles from Satellites; D. Wark, etc., M.W.R., June 66, pp 351-377.
2. An Analysis of Satellite Infrared Soundings at the Mesoscale Using Statistical Structure and Correlation Functions; D. Hillger, J.A.S., Feb. 79, pp 287-305.
3. Remote Sensing of Atmospheric Temperature Profiles with the Nimbus 5 Microwave Spectrometer; J. Waters, J.A.S., Oct, 75, pp 1953-1969.
4. Vertical Resolution of Remotely Sounded Temperature Profiles with a priori Statistics; C. Rodgers, J.A.S., Apr, 76, pp 707-709.
5. Remote Sensing of Cloudy Atmospheres: I: Single Cloud Layer; M. Chahine, J.A.S., Feb. 74 pp 233-243; II: Multiple Cloud Layers; M. Chahine, J.A.S. May 77, pp 744-757.
6. An Experiment to Determine the Value of Satellite Infrared Spectrometer (SIRS) Data in Numerical Forecasting; M. Atkins, etc., Meteorology Magazine, May 75, pp 125-142.
7. Interpretation of Satellite Cloud Mosaics for Southern Hemisphere Analysis and Reference Level Specification; G. Kelly, M.W.R., June 78, pp 870-889.
8. Four-Dimensional Data Assimilation Experiments in the Southern Hemisphere; D. Gaintlett, etc., J.A.M., Dec. 74, pp 845-853.
9. Experiments in Four Data Assimilation of Nimbus 4 SIRS Data; C. Hayden, J.A.M., April 73.
10. The Use of Surface Synoptic Data to Estimate Upper Level Humidity; R. Jonas, Meteorological Magazine, 1976, pp 44-56.
11. An Improved Satellite Nephanalysis Over the Sea; R. Harris, Meteorological Magazine, 1975, pp 9-17.
12. Satellite Viewed Jet Stream Clouds in Relation to Observed Wind Field; W. Vizee, J.A.M., Oct. 67, pp 929-935.
13. Temperature Retrieval from Satellite Radiance Measurement - An Empirical Method; S. Fritz, J.A.M., Feb. 77, pp 172-176.
14. Accuracy and Coverage of Temperature Data Derived from IR Radiometer on the NOAA 2 Satellite; R. Jastrow, etc., J.A.S., July 73, pp 958-964.
15. Atmospheric Ice and Water Content Derived from Parameterization of Nimbus 6 High Resolution Infrared Sounder Data; R. Feddes, etc., J.A.M., April 78, pp 536-551.

REFERENCE (cont'd)

- 16, On the Resolution of Temperature Profile Fine Structure by NOAA Satellite Vertical Temperature Profile Radiometer; O. Thompson, Feb, 76, M.W.R., pp 118-126.
17. Jet Stream Meteorology; E. Reiter, Univ. of Chicago 1963.

APPENDIX

THEORY

An examination of the radiation spectrum as seen above the earth will reveal gaps (fig, 1) (3). However, higher resolution spectrometers can detect individual peaks (fig, 2) (1) in these gaps which result from various transitional states of the molecules. The radiances (I) from these peaks are a function of frequency and temperature:

$$I(\bar{\nu}, 0) \propto \int B[\bar{\nu}, T(p)] d\tau(\bar{\nu}, p)$$

where  $T$  = temperature,  $p$  = pressure,  $\bar{\nu}$  = frequency interval,  $\tau$  = transmittance and

$B(\bar{\nu}, T)$  is the mean transmittance in a given spectral interval which is approximated by Rayleigh-Jeans Law in the microwave region or Wiens Law in the infrared region. The presence of water vapor causes additional absorption thus further complicating the estimate of the transmittance,

A gas produces a unique spectrum for a given pressure and temperature. Figure 2(1) illustrates a part of the CO<sub>2</sub> spectrum (15 micron carbon dioxide band). As CO<sub>2</sub> is distributed throughout the atmosphere, the spectrum will peak at a certain frequency for a given interval of the atmosphere. Figure 3 (2) illustrates where certain peaks dominate the spectrum for a given range of atmospheric pressures using the standard ICAO atmosphere. In addition to the CO<sub>2</sub> band, new technology now allows for microwave sensors to detect radiances from oxygen rotational bands, ice crystal, etc. Figure 4(4) is equivalent to figure 3 but deals with microwave radiation associated with oxygen. The longer wavelengths of microwave are less affected by cloud and moisture and allows for a better determination of the transmittance.

At present, VTPR is arrived by measuring radiance several times about an area under examination. Using sophisticated mathematical techniques (5, 6), the solution is made to converge towards a radiance value as seen through a clear atmospheric column. With improved technology such as increased spectral ranges, smaller scanning windows, etc., it will be possible to obtain, besides temperature profiles, estimates of cloud thickness, levels, and liquid water content (17).